First-Sphere and Second-Sphere Electrostatic Effects in the Active Site of a Class Mu Glutathione Transferase[†,‡]

Gaoyi Xiao,[§,||] Suxing Liu,[§] Xinhua Ji,[||,⊥] William W. Johnson,[§] Jihong Chen,[§,#] James F. Parsons,[§,#] Walter J. Stevens,[||,⊥] Gary L. Gilliland,*[,||,⊥] and Richard N. Armstrong*[,§,#]

Department of Chemistry and Biochemistry, University of Maryland, College Park, Maryland 20742, Center for Advanced Research in Biotechnology of the Maryland Biotechnology Institute, University of Maryland, Shady Grove, and of the National Institute of Standards and Technology, 9600 Gudelsky Drive, Rockville, Maryland 20850, and Department of Biochemistry and Center in Molecular Toxicology, Vanderbilt University School of Medicine, Nashville, Tennessee 37232-0146

Received January 25, 1996; Revised Manuscript Received February 27, 1996[⊗]

ABSTRACT: The activation of the thiol of glutathione (GSH) bound in the active site of the class mu glutathione transferase M1-1 from rat involves a hydrogen-bonding network that includes a direct (first-sphere) interaction between the hydroxyl group of Y6 and the sulfur of GSH and second-sphere interactions involving a hydrogen bond between the main-chain amide N-H of L12 and the hydroxyl group of Y6 and an on-face hydrogen bond between the hydroxyl group of T13 and the π-electron cloud of Y6 (i.e., T13-OH- - -π-Y6-OH- - -$^{-}$SG). The functions of these hydrogen bonds have been examined with a combination of site-specific mutagenesis and X-ray crystallography. The hydroxyl group of Y6 has a normal pK_a of about 10 even though it is shielded from solvent and is in a largely hydrophobic environment. The apparent pK_a of GSH in the binary Y6F·GSH complex is increased by 1.6 log units, and the reactivity of the enzyme-bound nucleophile is reduced. The catalytic properties of the Y6L mutant are identical to those of Y6F, suggesting that the weakly polar on-edge interaction between the aromatic ring and sulfur has no influence on catalysis. The refined three-dimensional structure of the Y6F mutant in complex with GSH shows no major structural perturbation of the protein other than a change in the coordination environment of the sulfur. Removal of the second-sphere influence of the on-face hydrogen bond between the hydroxyl group of T13 as in the T13V and T13A mutants elevates the pK_a of enzyme-bound GSH by about 0.7 pK_a units. Crystal structures of these mutants show that structural changes in the active site are minor and suggest that the changes in pK_a of E·GSH are due to the presence or absence of the on-face hydrogen bond. The T13S mutant has a completely different side-chain hydrogen-bonding geometry than T13 in the native enzyme and catalytic properties similar to the T13A and T13V mutants consistent with the absence of an on-face hydrogen bond. The γ-methyl group of T13 is essential in enforcing the on-face hydrogen bond geometry and preventing the hydroxyl group from forming more favorable conventional hydrogen bonds.

The glutathione (GSH)[1] S-transferases catalyze the addition of the thiolate of glutathione to substrates bearing electrophilic functional groups. One of the central issues in the catalytic mechanism of the enzyme is how the protein enhances the reactivity of the thiol of GSH. Spectroscopic and kinetic studies of the class mu isoenzyme M1-1[2] from rat suggest that the pK_a of GSH in the binary (E·GSH) complex is 6.2−6.7 or almost three pK_a units lower than that of GSH in aqueous solution (Liu et al., 1992). How the enzyme accomplishes this for a thiol that has restricted access to solvent is not fully understood. Fortunately, the three-dimensional structure of a binary E·GSH complex is known for the M1-1 isoenzyme from rat (Ji et al., 1992). Although the interactions between the sulfur of GSH in the active sites of various isoenzymes surely differ in detail, many of the basic features are conserved (Armstrong, 1994; Dirr et al., 1994; Wilce & Parker, 1994).

The immediate environment of the sulfur atom in the E·GSH complex consists of several first-sphere interactions with the protein and associated solvent. Virtually all cytosolic GSH transferases have a conserved tyrosine residue (Y6 of M1-1) the hydroxyl group of which appears, in most crystal structures, to be within hydrogen-bonding distance of the sulfur atom of the tripeptide (Figure 1) (Ji et al., 1992, 1993, 1994, 1995; Garcia-Saez et al., 1994; Reinemer et al., 1991, 1992; Sinning et al., 1993). This specific interaction has been suggested to be responsible, in large part, for the low pK_a of GSH in the E·GSH complex. Removal of this interaction by site-specific mutagenesis as in the Y6F mutant of M1-1 (Liu et al., 1992) or in other isoenzymes impairs the catalytic efficiency of the protein and raises the apparent

[†] This work was supported by National Institutes of Health Grant GM30910.

[‡] The final coordinates for the structures of the native and mutant enzymes have been deposited with the Brookhaven Protein Data Bank under the file names 6GST, 6GSU, 6GSV, 6GSW, 6GSX, and 6GSY.

* Address correspondence to these authors.
[§] University of Maryland, College Park.
[||] Center for Advanced Research in Biotechnology.
[⊥] National Institute of Standards and Technology.
[#] Present address: Vanderbilt University.

[⊗] Abstract published in *Advance ACS Abstracts,* April 1, 1996.

[1] Abbreviations: GSH, glutathione; CDNB, 1-chloro-2,4-dinitrobenzene; GSP, (9*R*,10*R*)-9-(*S*-glutathionyl)-10-hydroxy-9,10-dihydrophenanthrene; EDTA, ethylenediaminetetraacetic acid; Tris; tris(hydroxymethyl)aminomethane.

[2] This nomenclature is derived from that recently recommended by Mannervik et al. (1992).

0006-2960/96/0435-4753$12.00/0

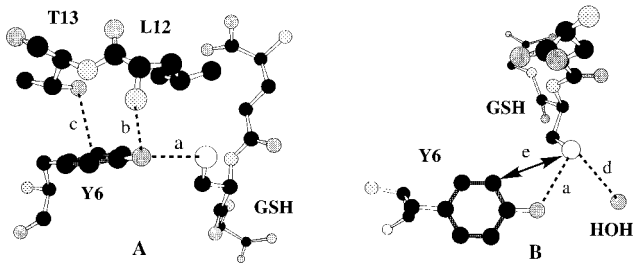

FIGURE 1: Two views of the hydrogen-bonding network in the complex of isoenzyme M1-1 and GS^-. View A is in the plane of the aromatic ring of Y6 and shows the hydrogen bonds between (a) the -OH of Y6 and the sulfur of glutathione, (b) the amide NH of L12 and the -OH of Y6, and (c) the -OH of T13 and the π-electron cloud of Y6. View B is from one face of the aromatic ring and shows (a) the hydrogen bond between the -OH of Y6 and the sulfur, (d) a solvent molecule (H_2O or NH_4^+) associated with the sulfur, and (e) the close (3.9 Å) van der Waals contact between the sulfur and the electropositive edge of the aromatic ring of Y6. Carbon, oxygen, nitrogen and sulfur atoms are shown in black, dark gray, light gray, and white, respectively.

pK_a of the enzyme-bound thiol (Liu et al., 1992). The only other hydrogen-bonding interactions with the sulfur are with one or two water molecules in the solvation shell. The sulfur is nestled against the side chain of L12 and the edge of the aromatic ring of Y6. These two van der Waals interactions shield a large portion of the sulfur atom from solvent.

In addition to the first-sphere interactions involving the tyrosyl residue in the active site, there are second-sphere interactions that may also influence the electrostatic environment of the sulfur. The most notable of these are an on-face hydrogen bond between the hydroxyl group of T13 and the π-electron cloud of Y6 (Liu et al., 1993) and a hydrogen bond between the main-chain NH of L12 and the hydroxyl group of Y6 (see Figure 1). A preliminary investigation of the on-face hydrogen bond suggests that it contributes about 4 kJ/mol (1 kcal/mol) to the stability of the thiolate (GS^-) in the active site (Liu et al., 1993). Long before the crystal structures of GSH transferases were reported it was speculated that part of the electrostatic field that contributes to the stability of the thiolate might be the N-terminal end of a helix dipole (Chen et al., 1988). The N-terminal end of the α1 helix does indeed point toward the active site, but the sulfur atom of GSH appears to be improperly oriented and too far away for the helix dipole to have a direct influence on the ionization behavior of the thiol. Nevertheless, it has been argued, based on semiempirical electrostatic calculations, that the α1 helix dipole in the class pi isoenzyme has a substantial effect on the pK_a of the tyrosyl hydroxyl group (Karshikoff et al., 1993). The role of the helix dipole in the M1-1 isoenzyme is unclear in this regard. However, one dipolar interaction that may very well influence the electronic properties of the hydroxyl group of Y6 is the hydrogen bond donated by the main-chain NH of L12 (Figure 1).

In this paper we report a mechanistic and structural evaluation of both first- and second-sphere interactions in the active site of a class mu GSH transferase that influence the apparent acidity and reactivity of the enzyme-bound sulfur. The refined three-dimensional structure of the Y6F mutant in complex with GSH shows no major structural perturbation of the protein other than a change in the coordination environment of the sulfur. This change is associated with an elevation of the pK_a and a decrease in reactivity of the enzyme-bound thiol. Ultraviolet−visible difference spectroscopy between the native enzyme and the Y6F mutant suggests that the hydroxyl group of Y6 in the native enzyme has a relatively normal pK_a. Removal of the second-sphere influence of the on-face hydrogen bond between the hydroxyl group of T13 as in the T13V and T13A mutants elevates the pK_a of enzyme-bound GSH by about 0.7 pK_a units. Crystal structures of these mutants show that structural changes in the active site are minor and suggest that the changes in pK_a of E·GSH are due to the presence or absence of the on-face hydrogen bond. The T13S mutant has a completely different side-chain hydrogen-bonding geometry than the native enzyme and catalytic properties similar to the T13A and T13V mutants consistent with the absence of an on-face hydrogen bond.

EXPERIMENTAL PROCEDURES

Site-Specific Mutants. The Y6F mutant was prepared as previously described by Liu et al. (1992). An expression plasmid, pGT33MXY6L, encoding the Y6L mutant was constructed in a manner analogous to Y6F by replacing the 30 base-pair cassette, between the *Nde*I and *Sac*II restriction sites, encoding the first nine amino acids with a synthetic duplex in which the TAC codon at position 6 was altered to TTA. Construction of expression plasmids pGT33MXT13A, pGT33MXT13V, and pGT33MXT13S encoding the T13A, T13V, and T13S mutants, respectively, under control of the λ promoter was also accomplished by cassette mutagenesis. The 30 base-pair cassette lying between the *Sac*II and *Xho*I restriction sites of pGT33MX was replaced with a synthetic linker of identical sequence except that the codon at position 13 was altered to GCA, GTA, and TCA to encode alanine, valine, and serine, respectively. This region of each recombinant clone was sequenced to ascertain if the desired mutation was present and that no other mutations had occurred during the manipulations. The mutant enzymes were expressed in and purified from *Escherichia coli* strain M5219 by the general method previously described (Zhang et al., 1991) for the native enzyme.

pH vs Rate Profiles. The dependence of the kinetic parameter k_{cat}/K_m^{CDNB} on pH was determined as previously described (Liu et al., 1992). Assays were performed at 25 °C with CDNB as the varied substrate and the concentration of GSH fixed at a saturating level of 2 mM. Under these conditions the pH dependence of the parameter k_{cat}/K_m^{CDNB} reflects ionizations in the E·GSH complex. The initial velocity data at each pH were analyzed with the program HYPER (Cleland, 1979) to obtain the kinetic parameters k_{cat} and k_{cat}/K_m^{CDNB}. The pH dependence of k_{cat}/K_m^{CDNB} was analyzed with the program HABELL (Cleland, 1979).

Spectrophotometric Titration of the Hydroxyl Group of Y6. The pK_a of the hydroxyl group of Y6 was estimated by UV difference spectroscopy in which the intensity of the absorption band for the tyrosinate anion at 256 nm was determined as a function of pH. Spectra were acquired on a Perkin-Elmer Lambda 18 spectrometer.[3] The spectra of identical concentrations of the native enzyme and the Y6F mutant were recorded, digitized, and stored at each pH using the buffer as reference. The difference spectrum (native − Y6F) was then calculated. The observed A_{256} was fitted to a sigmoidal function of pH to obtain the apparent pK_a of the hydroxyl group.

Ab Initio Calculations. Calculations of the geometry and energetics of the interaction of the sulfur with tyrosine and

phenylalanine were carried out as previously described (Liu et al., 1993). Glutathione, tyrosine, and phenylalanine were modeled using methanethiolate, *p*-cresol, and toluene, respectively. The initial geometry of each complex was constructed using the non-hydrogen coordinates of the refined crystal structures. The intramolecular coordinates of non-hydrogen atoms and the intermolecular bond angles and torsion angles were constrained to the crystal structure values. Optimizations of the proton positions and the hydrogen bond distances were carried out at the SCF level of theory with a 3-21G* Gaussian basis set. The geometry was optimized for deprotonated methanethiol interacting with the hydroxyl group of *p*-cresol and with the edge of toluene. Interaction energies were calculated in a second step at the SCF/MP2 level with a 6-31+G* basis set using the 3-21G* optimum geometry. The MP2 level of theory incorporates electron correlation effects including dispersion, and the large basis set provides a satisfactory description of the electrostatic properties of the molecules in the complex, including the methanethiolate anion. The interaction energies were corrected for basis set superposition effects using the counterpoise method (Boys & Bernardi, 1970). All calculations were performed with *Gaussian 92*, Revision A (Frisch et al., 1992).

Crystallization of Mutants. Crystals of the mutant enzymes were prepared essentially as described for the native protein (Ji et al., 1992). Crystals were grown in sitting drops which initially consisted of between 8 and 12 mg/mL protein in 25 mM Tris buffer (pH 8.0) containing 1 mM EDTA, 0.2% β-octyl D-glucopyranoside, 2 mM of the product inhibitor (9*R*,10*R*)-9-*S*-glutathionyl-10-hydroxy-9,10-dihydrophenanthrene (GSP), and buffered (pH 8) ammonium sulfate at 40−50% saturation. The drops were equilibrated at room temperature against wells containing between 60% and 72% saturated ammonium sulfate in 25 mM Tris buffer (pH 8.0). This procedure gave crystals of the same habit as the native enzyme (space group *C*2) in 5−10 days. Crystals of the Y6F·GSH complex were grown under similar conditions except GSH was substituted for the product inhibitor.

X-ray Diffraction Data Collection. X-ray diffraction data were collected from single crystals of mutant enzymes of T13A, T13V, T13S, and Y6F complexed with (9*R*,10*R*)-9-(*S*-glutathionyl)-10-hydroxy-9,10-dihydrophenanthrene (GSP) or glutathione (GSH) in the case of Y6F·GSH using a Siemens electronic area detector and Rigaku rotating anode X-ray source, as previously described (Ji et al., 1992). For crystals of mutants T13A, T13V, and Y6F, data collection was carried out at well controlled room temperature (20 ± 1 °C). Crystals were mounted in thin-walled glass capillaries with diameters of 0.7 or 1.0 mm, depending upon the size of crystals. For small crystals of the T13S mutant initial data collection as described above yielded data to 2.7 Å resolution. The resolution was extended to 2.4 Å using similar size crystals and a synchrotron source (station X8C at Brookhaven Synchrotronic Beamline). For the studies reported here, data were extended to 1.75 Å by utilizing the following cryotechnique. The crystals of T13S were first soaked in a protectant solution containing 65% ammonium sulfate, 10 mM Tris buffer, and 10% glycerol for 10 min. They were then transferred to a solution containing 17% glycerol for additional 10 min. Finally, the crystals were soaked in protectant solution containing 25% glycerol for 2 min before they were placed on the gonistat. A single crystal was mounted on a nylon loop suitable for data collection at low temperature. The X-ray data were collected at −130 ± 2 °C using a modified Enraf-Nonius cryostat. All raw data frames were processed on an Indigo2 computer using the XENGEN suite of programs (Howard et al., 1987). All of the mutants crystallized in space group *C*2 and were isomorphous with crystals of the native enzyme. The parameters for data processing are presented in Table 1 for the five mutant enzymes.

Table 1: Summary of X-ray Data Processing for the Native and Mutant Enzymes in Complex with GSH or GSP

	M1-1· GSH	Y6F· GSH	Y6F· GSP	T13A· GSP	T13V· GSP	T13S· GSP[a]
unit cell						
a (Å)	87.98	87.84	87.84	88.24	88.53	86.63
b (Å)	69.41	69.70	69.22	69.44	69.28	68.54
c (Å)	81.34	81.57	81.32	81.28	81.41	80.37
β (deg)	106.07	105.38	105.90	106.01	105.74	105.18
data						
D_{min} (Å)	2.20	2.20	1.91	1.85	1.85	1.75
total data	87 470	90 863	92 958	149 364	135 610	187 981
unique data obsd	22 810	23 171	36 384	38 422	37 279	45 856
data with $I \geq 2\sigma(I)$	19 920	19 170	29 659	33 244	33 763	38 637[b]
R_w[c]	0.076	0.091	0.090	0.078	0.088	0.090
R_{uw}[d]	0.064	0.097	0.071	0.059	0.066	0.070

[a] Data collected at −130 °C. [b] Data with $I \geq 1.5\sigma(I)$. [c] The weighted least-squares *R* factor on intensity for symmetry-related observations: $R_w = \sum[(I_{ij} - G_{ij}\langle I\rangle_j)/\sigma_{ij}]^2/\sum(I_{ij}/\sigma_{ij})^2$ where $G_{ij} = g_i + A_i s_j + B_i s_j^2$; $s = \sin\theta/\lambda$; *g*, *A*, and *B* are scaling parameters. [d] The unweighted absolute *R* factor on intensities: $R_{uw} = \sum(I_{ij} - G_{ij}\langle I\rangle_j/\sum|I_{ij}|)$.

Crystallographic Refinement. The starting model for the refinements of the enzyme complexes M1-1·GSH, Y6F· GSH, Y6F·GSP, T13A· GSP, T13V· GSP, and T13S·GSP was the 1.8 Å resolution structure of the M1-1 isoenzyme complexed with (9*S*,10*S*)-9-(*S*-glutathionyl)-10-hydroxy-9,-10-dihydrophenanthrene (2GST) (Ji et al., 1994), after deletion of both inhibitors and all the solvent molecules. In each T13 mutant the side chain was initially replaced with an alanyl side chain. The refinements were performed on a CRAY-YMP computer with GPRLSA (Furey et al., 1982), a restrained least-squares refinement procedure (Hendrickson & Konnert 1980a,b; Hendrickson 1985a,b). The examination of $2F_o - F_c$, $F_o - F_c$, and omit maps, the adjustment of the models, and deletion and addition of water molecules employed the programs FRODO (Jones, 1978) and O (Jones et al., 1991; Jones & Kjeldgaard, 1993) implemented on an Evans & Sutherland PS390 graphics system and an Indigo2 workstation. The entire model was checked and adjusted when necessary. Water molecules and sulfate anions were located on the difference electron density maps as peaks higher than 3σ. Solvent molecules were incorporated in the model and verified by a series of omit maps (Furey, 1990) with about 100 water molecules deleted each time. This procedure was performed in ascending order starting from the bottom of the list of water molecules ranked according to the parameter OCC^2/B (James & Sielecki, 1983), the ratio

[3] Certain commercial equipment, instruments, and materials are identified in this paper in order to specify the experimental procedure as completely as possible. In no case does such identification imply a recommendation or endorsement by the National Institute of Standards and Technology nor does it imply that the material, instrument, or equipment identified is the best available for the purpose.

Table 2: Least-Squares Refinement Parameters for the Native and Mutant Enzymes Complexed with GSH and GSP

	M1-1·GSH	Y6F·GSH	Y6F·GSP	T13A·GSP	T13V·GSP	T13S·GSP
resolution range (Å)	6.00−2.20[a]	6.00−2.20[b]	6.00−1.91[b]	6.00−1.85[b]	6.00−1.85[b]	6.00−1.75[a]
crystallographic R[c] factor	0.149	0.168	0.152	0.175	0.163	0.181
number of residues	434	434	434	434	434	434
water molecules	420	402	448	322	324	474
sulfate ions	0	0	3	3	3	3
GSH or GSP molecules	2	2	2	2	2	2
RMS deviations (Å) from ideal						
bond distances	0.012	0.015	0.018	0.016	0.016	0.020
angle distances	0.033	0.039	0.037	0.036	0.036	0.039
planar 1−4 distances	0.032	0.038	0.043	0.033	0.036	0.043
planarity	0.019	0.024	0.023	0.020	0.022	0.024
chirality	0.189	0.233	0.225	0.193	0.206	0.232
thermal parameter correlation (mean/ΔB) (Å^2)						
main chain bond	0.704	0.824	0.953	0.912	0.851	0.960
main chain angle	1.229	1.413	1.575	1.421	1.360	1.465
side chain bond	1.210	1.420	1.779	1.609	1.647	1.832
side chain angle	1.926	2.209	2.798	2.384	2.521	2.583

[a] $I \geq 1.5\sigma(I)$. [b] $I \geq 2.0\sigma(I)$. [c] $R = \sum_{hkl}||F_o| - |F_c||/\sum_{hkl}|F_o|$.

of the square of the fractional occupancy factor (OCC) of the oxygen atom and the crystallographic temperature factor (B). Lower resolution diffraction data excluded from the refinement were included in all map calculations. The agreement between solvent molecules (i.e., within 1 Å) among the six structures varied but was >60% (62−78%) except for Y6F·GSH, where it was 43% due to a less accurate data set. Three sulfate ions were included in the refinement of the four higher (<2 Å) resolution structures. A summary of the crystallographic refinement is found in Table 2. The final coordinates for the structures of M1-1·GSH, T13A·GSP, T13V·GSP, T13S·GSP, Y6F·GSP, and Y6F·GSH, have been deposited in Brookhaven Protein Data Bank (Bernstein et al., 1977) under file names 6GST, 6GSU, 6GSV, 6GSW, 6GSX, and 6GSY, respectively.

RESULTS

Characteristics of the Active-Site Tyrosyl Residue. The proton affinity or pK_a of the tyrosyl hydroxyl group is of obvious interest for any analysis of the mechanism of the enzyme. There are 14 tyrosyl residues in the native M1-1 isoenzyme. The pK_a and spectral characteristics of Y6 were obtained by site-directed-mutant difference spectroscopy in which the signal for Y6 was isolated from the other 13 residues by using the Y6F mutant enzyme as the reference. The resulting difference spectrum should be, to a first approximation, the spectrum of Y6 minus the spectrum of F6. The characteristics of the difference spectrum at pH 6.5 (Figure 2) were consistent with a single, neutral tyrosyl side chain. At pH >8 absorption bands characteristic of the tyrosinate anion appear at 256 and 310 nm. Both bands are shifted 13−15 nm to the red of their normal energies in water of 243 and 295 nm, respectively. Red-shifts of this magnitude in the tyrosinate absorption bands indicate that the chromophore is located in an environment that is significantly less polar than water (Demchenko, 1986), a fact that is fully consistent with the solvent-restricted environment apparent in the three-dimensional structure. Nevertheless, the pH dependence of the appearance of the band at 256 nm suggests that the hydroxyl group of Y6 has a near normal pK_a of about 10 (Figure 2). The extinction coefficient of the 256 nm band is exactly that expected for a single ionized tyrosine. For comparative purposes a similar analysis of the

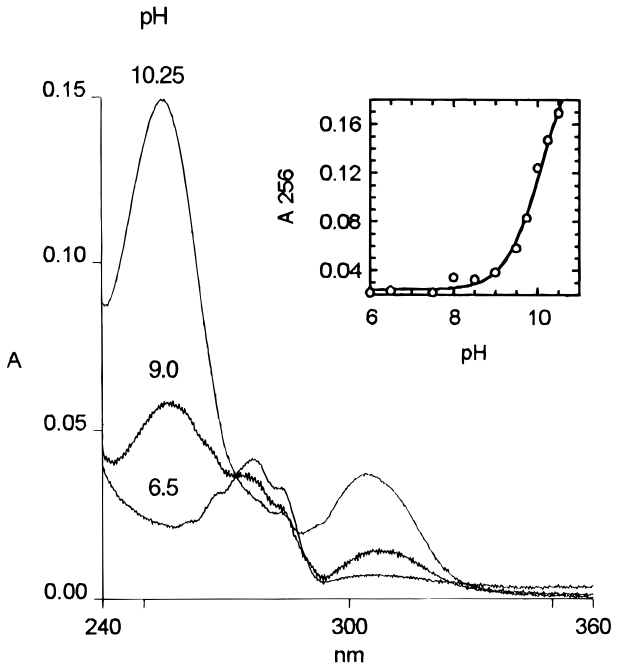

FIGURE 2: UV−visible difference spectra of the native enzyme and the Y6F mutant at pH 6.5, 9.0, and 10.25. Concentration of each enzyme was 21 μM active sites. (Inset) pH Dependence of the appearance of the tyrosinate absorption band at 256 nm in the UV−visible difference spectra of native enzyme − Y6F. The solid line is a regression fit of the experimental data to the equation $A_{256} = [A_L + A_H(K_a/H^+)]/(1 + K_a/H^+)$ using the program WAVL (Cleland, 1979), where $A_L = A_{256}$ at low pH, $A_H = A_{256}$ at high pH, H^+ is the hydronium ion concentration, and K_a is the acid dissociation constant. The pK_a and $\epsilon_{256} = A_H/[E]$ obtained from the regression analysis are 10.2 ± 0.2 and 11 500 M^{-1} cm^{-1}, respectively. A similar analysis of the band at 305−310 nm gave a pK_a = 10.0 ± 0.3 and an extinction coefficient of 2500 M^{-1} cm^{-1}.

characteristics of Y115, which is located near the active site about 10 Å from Y6 and closer to the surface of the protein, was carried out. The difference spectrum between the native enzyme and the Y115F mutant at neutral pH was that expected for a single neutral tyrosyl group (data not shown). Titration of the difference spectrum indicated that the hydroxyl group of Y115 has a pK_a = 10.5. Moreover, the tyrosinate absorption bands at 243 and 301 nm exhibit little or no red-shift as expected given the more solvent-accessible environment of Y115 (Johnson et al., 1993; Ji et al., 1994).

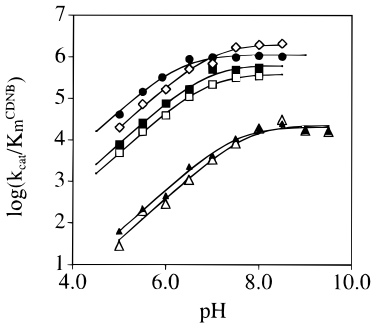

FIGURE 3: pH Dependence of k_{cat}/K_m^{CDNB} for native and mutant enzymes under conditions of saturating GSH. The solid lines are computer fits of the experimental data to the equation $\log(k_{cat}/K_m^{CDNB}) = \log[(k_{cat}/K_m^{lim})/(1 + [H^+]/K_a)]$. The experimental points, limiting values of k_{cat}/K_m^{CDNB} at high pH and the apparent pK_as derived from the computer fits for the enzymes are native M1-1 (●), $k_{cat}/K_m^{lim} = (1.1 \pm 0.1) \times 10^6$ M^{-1} s^{-1}, p$K_a = 6.3 \pm 0.2$; Y6F (△) $k_{cat}/K_m^{lim} = (2.3 \pm 0.4) \times 10^4$ M^{-1} s^{-1}, p$K_a = 7.8 \pm 0.3$; Y6L (▲), $k_{cat}/K_m^{lim} = (2.1 \pm 0.2) \times 10^4$ M^{-1} s^{-1}, p$K_a = 7.5 \pm 0.2$; T13A (□), $k_{cat}/K_m^{lim} = (3.9 \pm 0.2) \times 10^5$ M^{-1} s^{-1}, p$K_a = 6.9 \pm 0.1$; T13V (■), $k_{cat}/K_m^{lim} = (6.6 \pm 0.8) \times 10^5$ M^{-1} s^{-1}, p$K_a = 6.9 \pm 0.2$; T13S (◇), $k_{cat}/K_m^{lim} = (2.0 \pm 0.2) \times 10^6$ M^{-1} s^{-1}, p$K_a = 7.0 \pm 0.2$.

Properties and Structure of the Y6F Mutant. Removal of the hydroxyl group of Y6 as in the Y6F mutant has a marked effect on the catalytic properties of the enzyme as demonstrated by Liu et al. (1992). The pH dependence of k_{cat}/K_m^{CDNB} indicates that the apparent pK_a of the conjugate acid (E·GSH) of the nucleophile increases from about 6.2 in the native enzyme to 7.8 in Y6F·GSH and, contrary to expected Brønsted behavior, that k_{cat}/K_m^{CDNB} for the mutant on the high-pH plateau is less than that for the native enzyme (Figure 3). The apparent pK_a of Y6F·GSH remains significantly less than that of GSH in aqueous solution, which is about 9. These results suggest that there is a fundamental change in the mechanism or structure of the mutant enzyme. Moreover, it is clear that even in the absence of the hydroxyl group of Y6 the enzyme is capable of stabilizing the thiolate.

Crystals of Y6F in complex with either GSH or GSP were isomorphous with the native enzyme. The final $2F_o - F_c$ and $F_o - F_c$ electron density maps for both structures are fully consistent with the loss of the hydroxyl oxygen. In the case of Y6F·GSH, the final $2F_o - F_c$ and $F_o - F_c$ electron density maps reveal only glutathione at the active site as expected. Removal of the hydroxyl group of Y6 necessarily eliminates both the hydrogen-bonding interactions with the sulfur of GSH and the main-chain NH of L12 (Figure 1). In order to facilitate a detailed comparison of the native (M1-1·GSH) and Y6F·GSH complexes, the structure M1-1·GSH (1GST) was further refined using the more accurate geometry of 2GST. This resulted in a significant improvement in the crystallographic *R* factor which decreased from 0.171 to 0.149.

Superposition of the structure of M1-1·GSH and Y6F·GSH gives an overall RMS deviation on Cα positions of 0.24 Å and a local RMS deviation at the active site of 0.19 Å. The latter alignment is illustrated in Figure 4. When all 434 Cα-atoms of the enzymes are aligned, the average shift in positions of the Cα-atoms of GSH is 0.31 and 0.19 Å in subunits A and B, respectively. The sulfur atom moves 0.29 and 0.46 Å farther away from the aromatic ring of F6 in subunits A and B, reflecting the loss of the hydrogen bond with the hydroxyl group and a favorable van der Waals distance. The sulfur atom remains in the plane of the aromatic ring and is equidistant (4.0 Å) from the para carbon and the proximal meta carbon of F6. There are some small structural changes in the enzyme-bound GSH introduced by the mutation (Figure 4). Nevertheless, all other hydrogen bonds and salt bridges between the enzyme and GSH are present in the mutant.

Perhaps as significant as the loss of the hydrogen bond with Y6 is the fact that there is a decrease in crystallographically observable solvent molecules associated with the sulfur in the Y6F·GSH complex. In the native enzyme one water (or NH_4^+) is seen within hydrogen-bonding distance of the sulfur in subunit A while two are observed in subunit B. In contrast, there is one observable water (or NH_4^+), 3.2 Å away, in the inner coordination sphere of the sulfur in subunit A and none in subunit B. The thiol in the M1-1·GS^- complex (p$K_a = 6.2$) is clearly ionized at pH 8 where the crystal structure was determined. The thiol in the Y6F·GSH complex has an apparent p$K_a \geq 7.8$ (Liu et al., 1992), suggesting that it is about 50% ionized under the crystallographic conditions. The decrease in ordered solvent in the coordination environment of the sulfur may be a consequence of the much weaker hydrogen-bonding interactions between water (or NH_4^+) and the neutral species. It is interesting to note that the single water within hydrogen-bonding distance

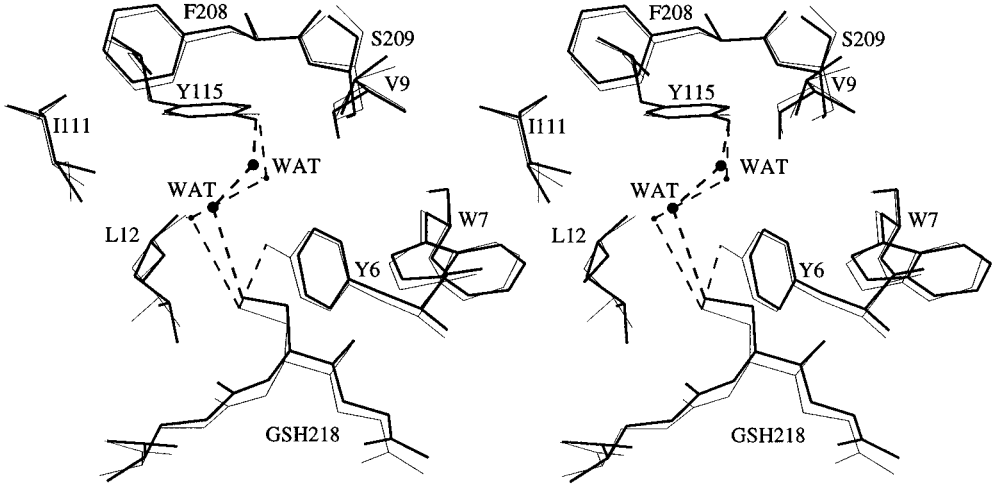

FIGURE 4: Stereoview of the alignment of the coordinates of the native enzyme in complex with GSH with the Y6F·GSH complex illustrated in the dark line.

of the sulfur in Y6F·GSH is in the plane of the aromatic ring and in van der Waals contact (4.2 Å) of the para carbon (CZ) of F6 almost as if it is a direct but more distant replacement for the missing hydroxyl group in the native enzyme.

Alignment of the Y6F mutant in which the active site is occupied with the thioether product (9*R*,10*R*)-9-*S*-glutathionyl-10-hydroxy-9,10-dihydrophenanthrene (GSP) with the structure of M1-1·GSP (PDB file 3GST) gives RMS deviations on Cα-positions of 0.14 Å. The only significant difference in the active sites of the two product complexes is the rotamer conformation adopted by the side chain of I111. An alignment of the two structures of the Y6F mutant gives an RMS deviation of Cα-positions of 0.23 Å. Thus, there are no global structural perturbations introduced either by the mutation or by the nature of the ligand. The small local differences between Y6F·GSH and Y6F·GSP are very similar to those found between M1-1·GSH (PDB file 1GST) and M1-1·GSP (PDB file 3GST).

On-Edge Interaction between GSH and F6. The sulfur of GSH in Y6F·GSH is nestled against the electropositive edge of the phenyl ring of F6. The extent to which this favorable, weakly polar electrostatic interaction might influence the stability and reactivity of the thiolate anion in the mutant was investigated. As expected, *ab initio* calculations of the strength of the on-edge interaction between methanethiolate and toluene in the gas phase gave a much smaller interaction energy, −21.4 kJ/mol (−5.1 kcal/mol) as compared to that of −75 kJ/mol (−17.9 kcal/mol) for the hydrogen-bonding interaction with the hydroxyl group of *p*-cresol (Liu et al., 1993). Although the calculated energies overestimate the strength of both interactions in the condensed phase where there is electrostatic shielding by solvent and other protein residues, the stabilization provided by the phenyl could be significant.

In order to ascertain whether the on-edge interaction between the thiolate anion and the electropositive edge of the aromatic ring of F6 might offer additional stabilization of the thiolate as compared to a van der Waals interaction with a nonaromatic group, the Y6L mutant was constructed, and its catalytic properties were evaluated. As indicated in Figure 3, the catalytic properties of Y6L are essentially indistinguishable from those of Y6F with respect to both the apparent pK_a of the bound thiol and the limiting value of k_{cat}/K_m^{CDNB}. Thus, the on-edge interaction appears to have no detectable kinetic significance in the enzyme-catalyzed reaction.

Catalytic Properties of T13 Mutants. One unique aspect of the electrostatics in the active site of the native enzyme is the on-face hydrogen bond between the hydroxyl group of T13 and the π-electron cloud of Y6. Removal of the on-face hydrogen bond in the T13A and T13V increases the apparent pK_a of enzyme-bound GSH by 0.7 log units (Figure 3). *Ab initio* calculations on a model system suggest this behavior is due to an increased proton affinity of the hydroxyl group of Y6, a decreased hydrogen bond strength to sulfur, and a decreased stability of the thiolate upon removal of the on-face hydrogen bond (Liu et al., 1993). The electrostatic attraction of the on-face hydrogen bond [calculated to be −19.6 kJ/mol (−4.7 kcal/mol) in the gas phase] suggests that the hydroxyl group of a serine residue at position 13 might also participate in an on-face hydrogen bond. If true, the T13S mutant would be expected to have catalytic properties similar to the native enzyme. This is not the case. The pH dependence of k_{cat}/K_m^{CDNB} for the T13S mutant (Figure 3) indicates that the apparent pK_a of the enzyme-bound thiol is 7.0 ± 0.2 and more closely resembles that observed for T13A·GSH and T13V·GSH (pK_a = 6.9). Either the on-face hydrogen bond is not present in the T13S mutant or the native M1-1·GSH complex exhibits a lower apparent pK_a for some other reason as discussed below.

Structures of T13 Mutants. To better understand the catalytic and structural ramifications of the on-face hydrogen bond, the three-dimensional structures of T13A, T13V, and T13S in complex with GSP were determined. The structures of the product complexes rather than the more relevant mutant·GSH complexes were determined because crystals of the enzyme·GSH complexes are generally more difficult to grow and do not diffract as well as the product complexes. Replacement of both the hydroxyl group and the γ-methyl group with hydrogen as in the T13A mutant would tend to reduce steric crowding near Y6 whereas replacement of the hydroxyl group with a methyl group as in T13V would increase steric crowding slightly by substituting a repulsive van der Waals contact for the attractive electrostatic contact of the on-face hydrogen bond.

The side chain of A13 in the T13A mutant is well defined in the final $2F_o - F_c$ electron density map as shown in Figure 5a. Local structural alignments of the C_α-atoms gives an RMS deviation of 0.22 Å for residues near the site of mutation (Figure 6a) and 0.20 Å for residues in the electrophilic substrate binding site (Figure 7a). The C_β-atom of A13 moves 0.53 Å toward the face of Y6 due to the smaller size of the side chain. This movement results in a slight shift of the backbone of the loop bearing A13. Consequently, the movement of the adjacent residue, L12, allows more room for the dihydrophenanthrenyl ring system which tilts toward L12 through changes in the torsion angles about the two thioether bonds. This movement in turn alters the side-chain conformation of I111 in the xenobiotic substrate binding site. In spite of these conformational differences, the positions of the sulfur atom and the crucial active site residues Y6 and Y115 do not change.

The final $2F_o - F_c$ electron density map of the T13V mutant is fully consistent with the presence of a valine side chain (Figure 5b). Changes in the position of the backbone near V13 are insignificant due to the comparable size of the V and T side chains. The local RMS deviations on C_α-positions is only 0.11 Å between the mutant and native structures. However, there is a rotation of 142° in χ for the side chain in T13V which prevents unfavorable van der Waals contact between the C_γ-carbons of the valine and the aromatic ring of Y6. Thus, the only significant conformational change in the T13V mutant is confined to the side chain of the mutated residue.

In principle, a seryl side chain at position 13 is capable of donating an on-face hydrogen bond to the aromatic ring of Y6. To avoid any model bias in determining the conformation of S13, the residue at position 13 was replaced by alanine in the starting model for the refinement of T13S mutant. The final omit $F_o - F_c$ electron density map contoured at 3σ (Figure 5c) and the final $2F_o - F_c$ electron density map contoured at 1σ (Figure 5d) unambiguously indicate that the side chain of S13 does not adopt a conformation for an on-face hydrogen bond as occurs in the native structure. Rather, it is positioned to participate in more conventional hydrogen

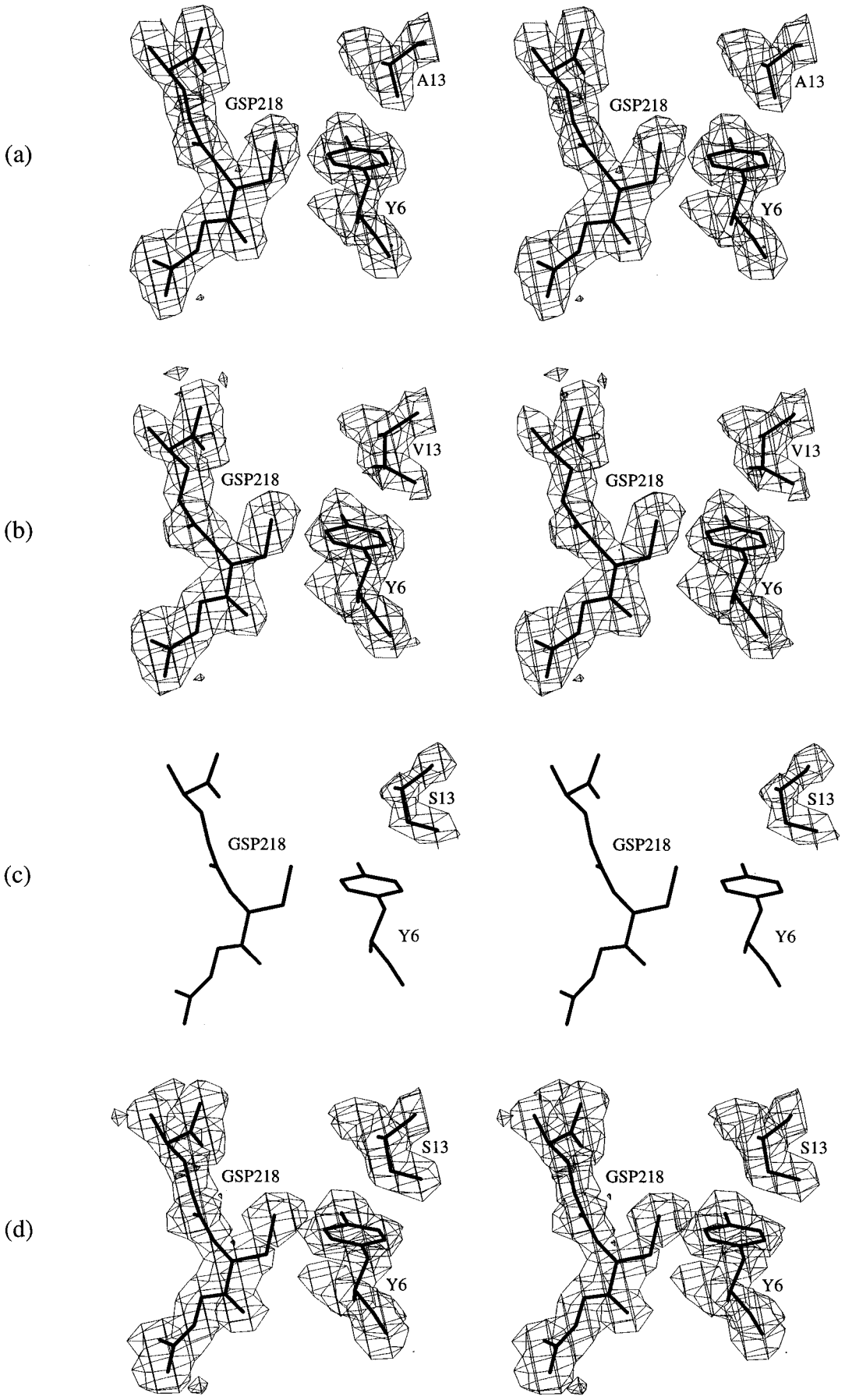

FIGURE 5: Stereoview of the final electron density maps for the T13 mutants: (a) $2F_o - F_c$ contoured at 1.0σ for T13A; (b) $2F_o - F_c$ contoured at 1.0σ for T13V; (c) $F_o - F_c$ contoured at 3.0σ for T13S; and (d) $2F_o - F_c$ contoured at 1.0σ for T13S. The dihydrophenanthrenyl portion is not shown in the maps for clarity.

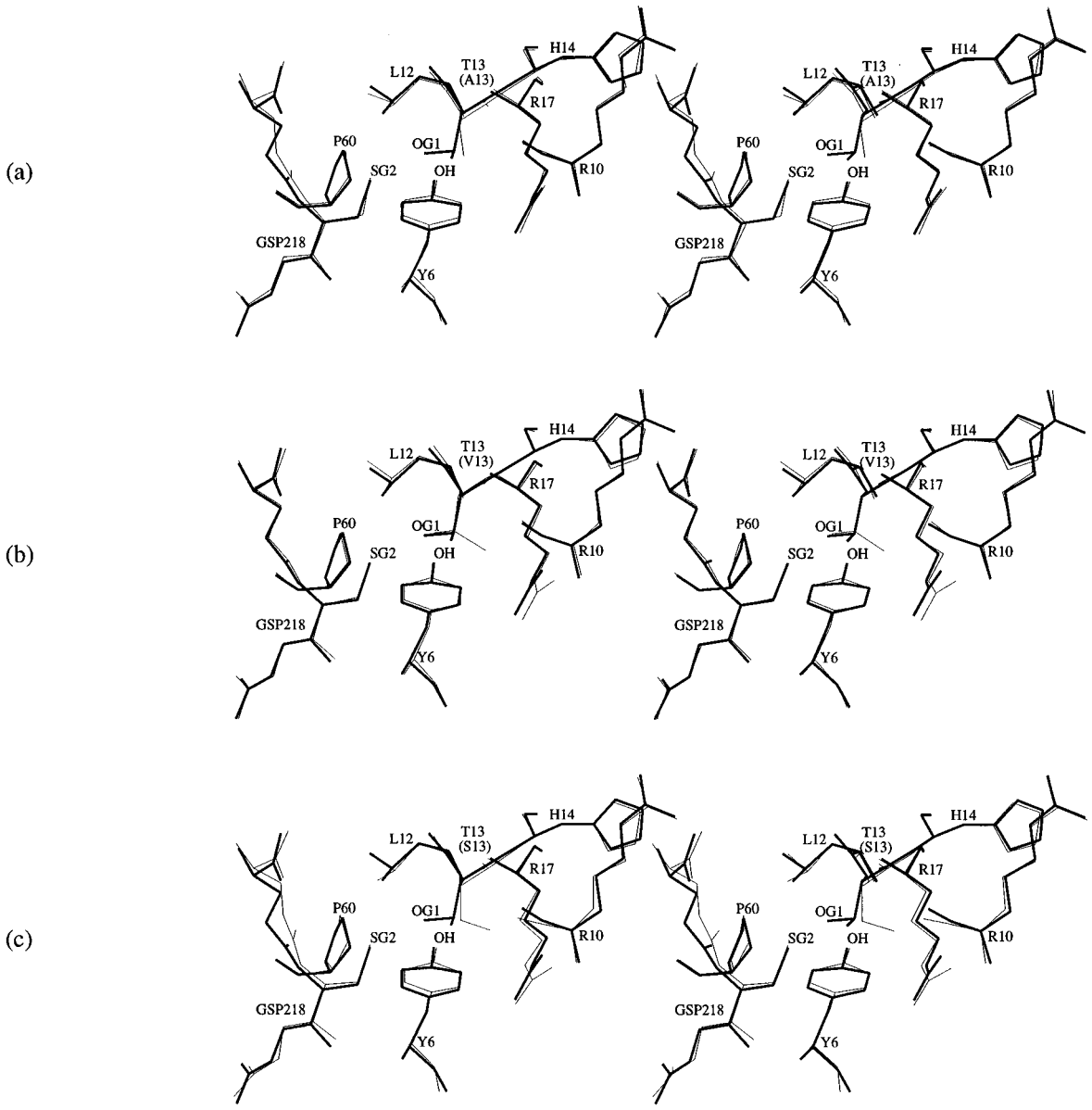

FIGURE 6: Stereoviews of the comparisons the native M1-1·GSP complex (3GST) with the mutants in complex with GSP near the site of mutation. The dihydrophenanthrenyl portion of the product is not shown for clarity. The native structure is shown in the dark line. (a) T13A, (b) T13V, and (c) T13S.

bonds with neighboring residues. In fact, the hydroxyl group of S13 appears to act as a hydrogen bond donor to the carbonyl oxygen of R10 and as a hydrogen bond acceptor from NH1 of the side chain of R17 as indicated in Figure 8. This is true in both subunits. Distances between the O_γ of S13 and the carbonyl oxygen of R10 are 2.98 and 2.80 Å in subunits A and B, respectively. Similarly, the distances between O_γ and NH1 of R17 are 2.98 and 3.11 Å for the two subunits.

The local structural alignments of the C_α-carbons between the three T13 mutants and the native structure indicates that the T13A mutation introduces the largest perturbation in the backbone structure while the T13V mutant introduces the least. This observation is readily understood by considering the relative size of the mutant side chains with respect to the native enzyme. The overall structural alignments of all 434 α-carbons of the three mutants and the native enzyme indicate RMS deviations of 0.15, 0.12, and 0.24 Å for T13A, T13V, and T13S, respectively, which are within experimental error for independently determined structures.

DISCUSSION

First-Sphere Interactions—Electrophilic Stabilization or General-Base Catalysis? There are two views as to the role of the hydroxyl group of Y6 (or its equivalent) in catalysis. One view is that the hydroxyl group acts as a hydrogen bond donor to the sulfur of enzyme-bound GSH (or GS^-) which lowers the pK_a of the enzyme-bound peptide (Liu et al., 1992). The alternative view is that the active site tyrosyl residue has an abnormally low pK_a as has been suggested for the class alpha and pi enzymes (Atkins et al., 1993; Karshikoff et al., 1993) and may therefore act as a general base to abstract the proton from GSH. It is important to distinguish the simple formation of the binary $E{\cdot}GS^-$ complex and its subsequent reaction with an electrophilic substrate in any discussion of the catalytic mechanism.

General base catalysis is certainly not an apt description of the participation of the tyrosyl hydroxyl group in the class mu enzyme either in the binding of the peptide or in addition of the sulfur to an electrophilic substrate and may not be

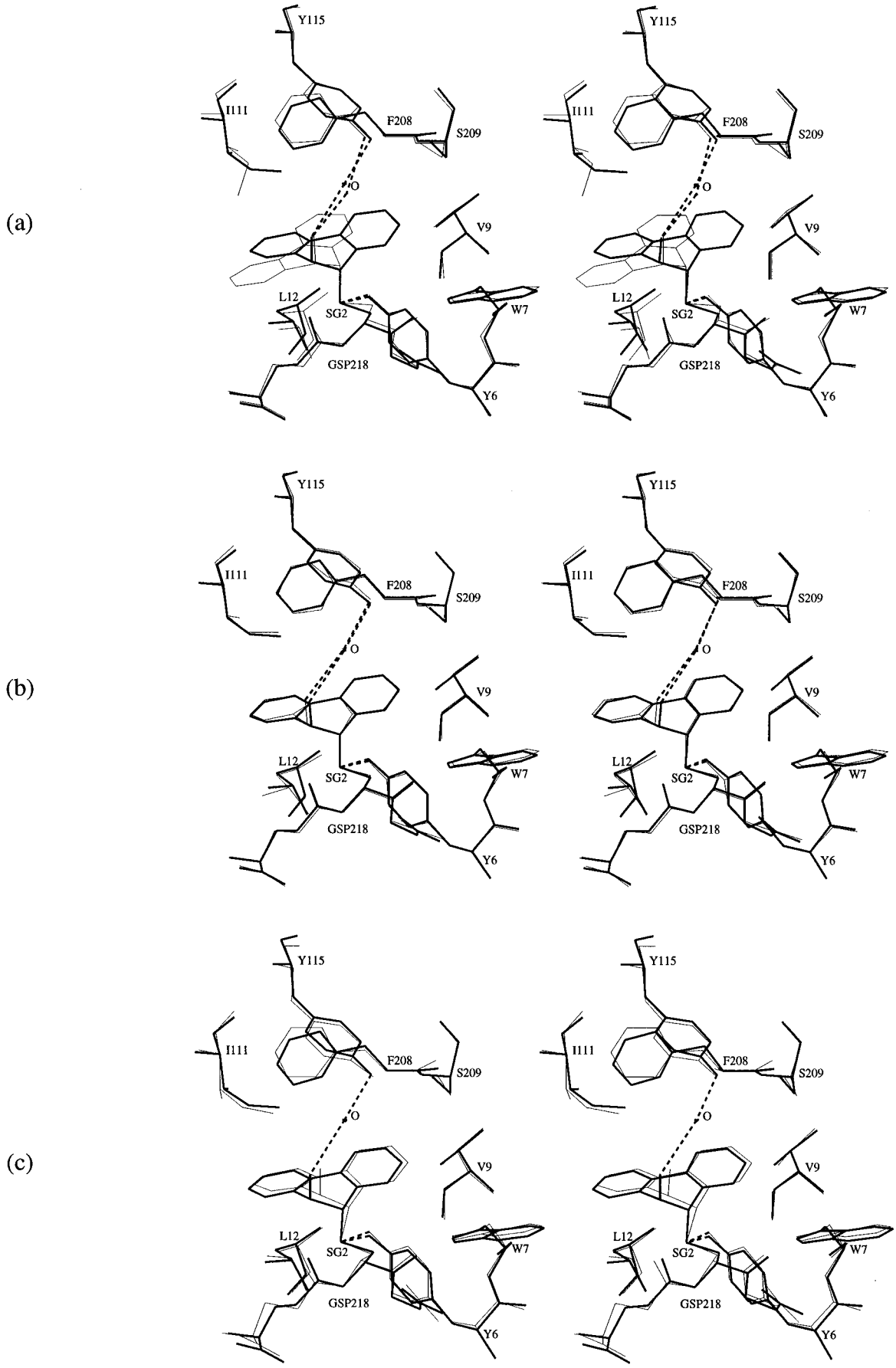

FIGURE 7: Stereoviews of the comparisons the native M1-1·GSP complex (3GST) with the mutants in complex with GSP near the xenobiotic substrate binding site. The native structure is shown in the dark line. (a) T13A, (b) T13V, and (c) T13S.

appropriate for the other enzyme classes as well. The pK_a of 10.2 for the hydroxyl group of Y6 is about the same as that expected in aqueous solution in spite of the fact that it is located in a solvent-restricted environment. The hydrogen

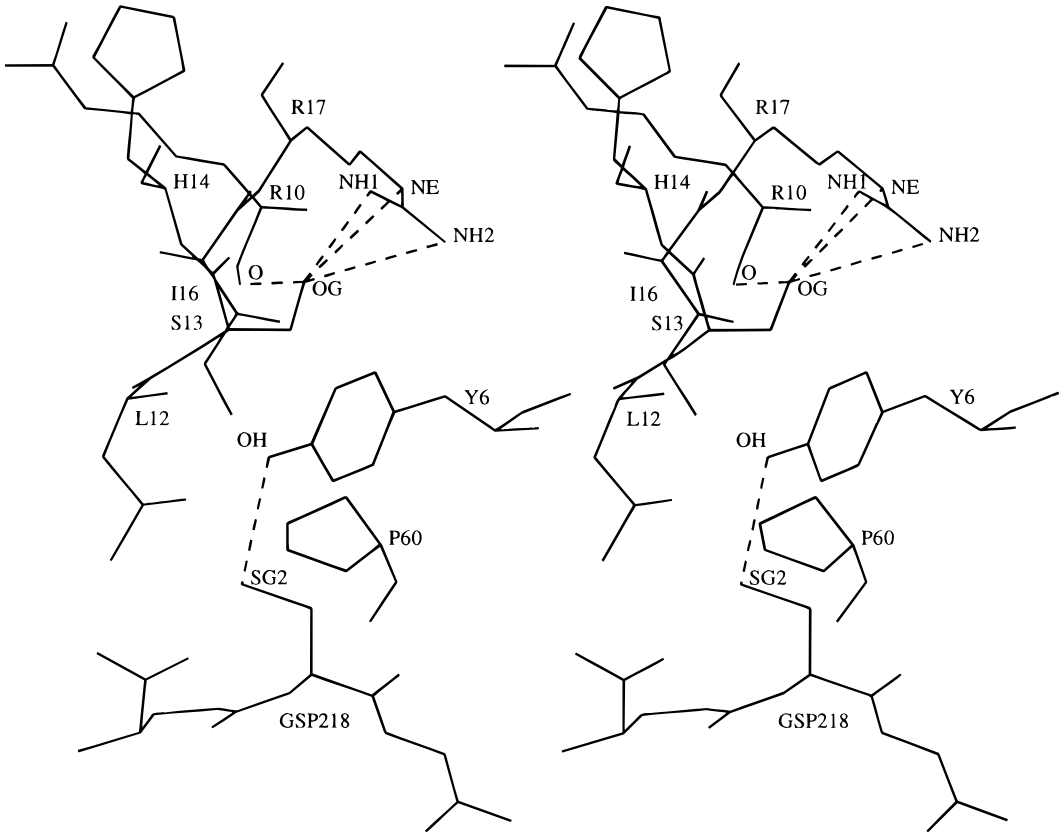

FIGURE 8: Stereoview of the alternative hydrogen-bonding network for the hydroxyl group of serine in the T13S mutant. The dihydrophenanthrenyl portion of the product is not shown for the sake of clarity.

Scheme 1

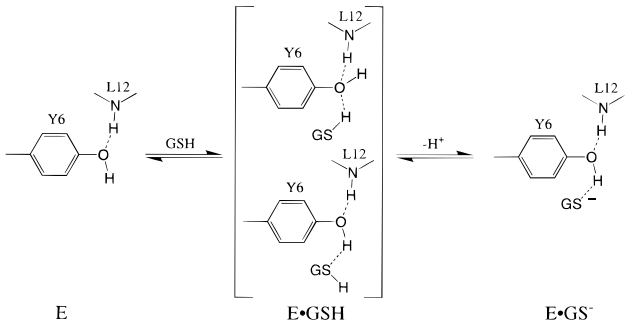

bond to the main chain NH of L12 (Figure 1) would tend to lower the pK_a of the hydroxyl group and probably accounts, in large measure, for the fact that the pK_a is not higher. Although it can be argued that a value of 10.2 is abnormally low for the pK_a of a phenolic hydroxyl group in a hydrophobic environment, it is clear that the group is predominantly protonated near physiologic pH. The fact that anionic inhibitors bind much more tightly to the class mu enzymes than does GSH (Graminski et al., 1989) is *prima facie* evidence that the hydroxyl group is not ionized. Both of these experimental observations argue that an ionized Y6 does not participate as a base for the removal of the thiol proton on binding GSH as suggested by Karshikoff et al. (1993).

The protonation states of the unliganded enzyme, E, and the binary E·GS$^-$ complex (Scheme 1) for the class mu enzyme are fairly clear from the spectroscopic evidence provided here and elsewhere (Liu et al., 1992). What is less clear is the configuration of the diprotonated species, E·GSH. One or the other configuration should resemble the transition state for proton loss. The bottom species in which Y6 acts as a hydrogen bond donor to sulfur perhaps provides more dispersal of the developing charge on sulfur. In either case a proton must be lost to solvent to generate the reactive species for nucleophilic attack.

The nature of the hydrogen bond in the reactive E·GS$^-$ complex is of some interest. The spectroscopic observation of the thiolate (Graminski et al., 1989; Liu et al., 1992) suggests that the proton is located principally on the oxygen of Y6 as indicated in Scheme 1. Moreover, this is the most reasonable scenario from the standpoint of simple electrostatics and chemical catalysis. The possibility of a short, strong (or low barrier) hydrogen bond between the hydroxyl group and the thiolate either in the ground state or transition state for nucleophilic addition seems unlikely. Kinetic solvent deuterium isotope effects on k_{cat}/K_m^{CDNB} for the addition of GSH to CDNB catalyzed by class alpha and mu enzymes are 0.8 (Huskey et al., 1991) and 0.9 (Parsons & Armstrong, 1996), respectively. A normal hydrogen bond in the ground state developing into a short, strong hydrogen bond or proton in flight in the transition state would be expected to give a substantial inverse solvent isotope effect, $k^H/k^D \leq 0.5$. In contrast, a short, strong hydrogen bond in the ground state that is dissipated before the transition state should give a large normal isotope effect, $k^H/k^D \geq 2$. Finally, low barrier hydrogen bonds in both the ground state and transition state would be predicted to exhibit a small normal isotope effect $k^H/k^D \geq 1$. None of these expectations are consistent with the modest inverse solvent isotope effects observed.

Finally, it is worth noting that there is a now a model for general base catalysis in a GSH transferase catalyzed reaction. The M1-1 isoenzyme in which the tyrosyl residues

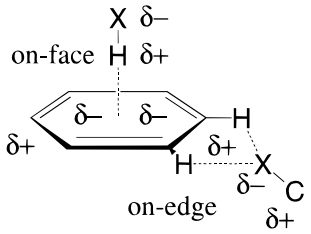

FIGURE 9: Illustration of weakly polar interactions of the quadrapole of an aromatic ring with electropositive and electronegative groups.

have been replaced with the unnatural amino acid 3-fluorotyrosine has unique catalytic properties attributed to the fact that the 3-fluorotyrosinate anion at position 6 ($pK_a = 7.5$ in the free enzyme) acts as a general base to remove the proton from GSH between the ground state and transition state for addition to CDNB (Parsons & Armstrong, 1996). In contrast to the native enzyme, the 3-fluorotyrosyl enzyme has a large inverse solvent deuterium isotope of 0.5 and a proton inventory that is consistent with a general base mechanism. The modest isotope effects observed with the native class alpha and mu enzymes are more consistent with the desolvation of a thiolate anion in the transition state for reaction (Huskey et al., 1991; Parsons & Armstrong, 1996) than with a general base mechanism.

Weakly Polar Electrostatic Interactions with Aromatic Residues. The electric quadrapole of an aromatic ring can, in principle, form favorable, though weak, electrostatic interactions with either electropositive or electronegative groups as illustrated in Figure 9. Weak electrostatic interactions involving hydrogen bond donors or cations and the electron-rich π-electron clouds of aromatic rings have been known for some time in protein structures (Wlodawer et al., 1984; Burley & Petsko, 1986, 1988; Singh & Thornton, 1990) and have been rigorously characterized in model systems (Suzuki et al., 1992; Rodham et al., 1993). Similarly, favorable interactions between electronegative groups and the electron-deficient edges of aromatic rings have been proposed (Thomas et al., 1982; Reid et al., 1985; Burley & Petsko; 1988). For the purposes of discussion we call these two types of weakly polar interactions on-face and on-edge interactions, respectively, as illustrated in Figure 9. Whether these enthalpically favorable interactions contribute in any substantial way to protein stability is not clear (Mitchell et al., 1994). Although functional roles for weakly polar interactions in binding and catalysis have been proposed (Sussman et al., 1991; Waksman et al., 1992; Cowan et al., 1993; Dougherty, 1996), there have been few experimental tests of the significance of such electrostatic effects (Liu et al., 1993; Jamison et al., 1995).

The structure of the M1-1 isoenzyme suggests that both on-edge and on-face interactions involving the active-site tyrosyl residue could have a measurable impact on the catalytic mechanism of the enzyme. The sulfur of GS^- is located in the plane of and is in van der Waals contact with the edge of the aromatic ring of Y6, a first-sphere interaction. Although the electrostatic interaction between Y6 and the thiolate is dominated by the hydrogen bond to the hydroxyl group, a small contribution of the electropositive edge of the ring to the stability of the thiolate is, in principle, possible. However, the comparable catalytic characteristics of the Y6F and Y6L mutants suggest that this is not the case in the Y6F mutant where an on-edge interaction should be more

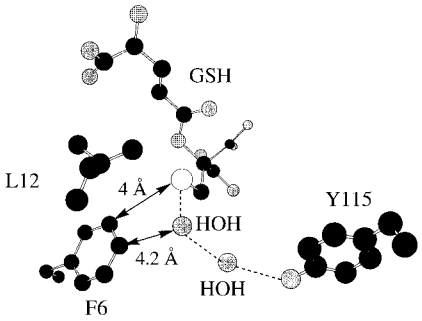

FIGURE 10: First-sphere interactions and the water network connecting the sulfur of GSH to the hydroxyl group of Y115 in the Y6F mutant. The figure is derived from the coordinates of subunit A in the crystal structure of the Y6F·GSH complex. Carbon, oxygen, nitrogen, and sulfur atoms are shown in black, dark gray, light gray, and white, respectively.

prominent. In contrast, an experimentally measurable second-sphere effect of the on-face hydrogen bond between T13 and Y6 has been demonstrated here and in preliminary work (Liu et al., 1993). The structural and mechanistic bases for these observations are discussed below.

First-Sphere and Second-Sphere Interactions in the Y6 Mutants. There are two curious aspects to the catalytic behavior of the Y6F mutant. The first is the fact that the apparent pK_a of the thiol in Y6F·GSH ($pK_a = 7.8$) is still lower than $GSH_{(aq)}$ ($pK_a = 9$) in aqueous solution in spite of the fact that the sulfhydryl group is partially desolvated by van der Waals contact with the edge of the phenyl ring and the side chain of L12. The second curiosity is that, contrary to normal Brønsted behavior, the thiolate of higher apparent basicity (Y6F·GS^-) is less reactive than M1-1·GS^- on the high-pH plateau.

What factors contribute to the lower than expected pK_a of the thiol in Y6F·GSH? The only crystallographically observable first-sphere interactions are the van der Waals contacts of the sulfur with the edge of F6 and the side chain of L12 and one hydrogen-bonded solvent molecule (subunit A) as illustrated in Figure 10. The possibility that an on-edge first-sphere interaction between the sulfur and the aromatic ring of F6 contributes to the stability of the thiolate can be ruled out given that the catalytic behavior of Y6L and Y6F is essentially identical. There are two possible explanations for the lower than expected pK_a. One possibility is that the apparent ionization observed in the pH profile is due to some group other than the thiol that acts as a general base to remove the thiol proton. In this regard, there are no ionizable groups in the vicinity of the sulfur that would be expected to have a pK_a near 8. The only direct hydrogen-bonding interaction is with the solvent molecule located 3.2 Å from the sulfur and 4.2 Å from the aromatic ring of F6 in subunit A (Figure 10). This solvent molecule, which appears to replace the missing hydroxyl group of Y6, is part of a network of solvent linking the sulfur to the hydroxyl group of Y115. However, the pK_a of Y115 is too high (10.5) to account for the ionization observed in the pH-rate profile. The pK_a of the first-sphere water molecule is expected to be even higher.

The second explanation is that second-sphere electrostatic effects are responsible for the additional stabilization of the thiolate. For example, in addition to the solvent molecules, the main-chain NH of L12 is 5.4 Å from the sulfur. Other microdipoles are found at distances of >6.5 Å and include

the hydroxyl groups of T13 (6.6 Å), Y115 (7.0 Å), and the main-chain NH of L59 (6.7 Å) and T13 (7.1 Å). Although the N-terminal end of the α1 helix dipole points toward the active site, the sulfur lies off the helix axis and is 8.5 Å from the first (H14) NH of the helix. The closest positively charged side chains are the guanidinium groups of R17, R49, and R107 located 9−10 Å from the sulfur and R10 at about 12 Å. Although none of the individual electrostatic interactions are particularly strong, their combined effect probably accounts for the enhanced stability of the thiolate in Y6F•GS^-.

What accounts for the lower than expected reactivity of the thiolate in Y6F•GS^-? The crystal structures of the Y6F mutant are of little help with respect to this issue. In the absence of any substantial structural changes in the active site, the anomalous (inverse) Brønsted behavior of the nucleophile can only be explained by a fundamental change in the character of the ground state or transition state for reaction in the mutant. One possibility is that desolvation of the nucleophile in the transition state is much more difficult in the absence of the hydroxyl group of Y6. The hydroxyl group of Y6 does not appear to provide for any particular orientation of the nucleophile but rather acts as a surrogate solvent molecule which enhances the desolvation of the reactive face of the sulfur.

Second-Sphere Effect of an Enforced On-Face Hydrogen Bond. Replacement of T13 with alanine, valine, or serine has a measurable effect on the apparent acidity of enzyme-bound GSH. That the increase in pK_a of 0.7 log units is due to the loss of the on-face hydrogen bond between T13 and Y6 and not some other perturbation of the electrostatics or structure of the active site is demonstrated by the fact that all three mutants T13A, T13V, and T13S exhibit the same shift in the pK_a of bound GSH and show no significant structural change in the interaction between the sulfur of the peptide and Y6.

The strengths of on-face hydrogen bonds are less than conventional hydrogen bonds between neutral donor−acceptor pairs (Levitt & Perutz, 1988; Burley & Petsko, 1988) and even less when compared to neutral-charged donor−acceptor pairs (Liu et al., 1993). Simple electrostatic potential energy calculations suggest that neutral NH−π interactions are worth approximately −12 kJ/mol (−3 kcal/mol) or about half the strength of conventional hydrogen bonds (Levitt & Perutz, 1988). The interaction energy for the on-face hydrogen bond between T13 and Y6 in the presence of the thiolate has been estimated to be at least 6.3 kJ/mol (−1.5 kcal/mol) but certainly less than the −19.6 kJ/mol (−4.5 kcal/mol) obtained from high-level *ab initio* calculations in the gas phase (Liu et al., 1993).

In spite of favorable interaction energies, weakly polar interactions cannot compete effectively with multiple and stronger, more conventional dipole−dipole or charge−dipole interactions. This point is most clearly illustrated by the preference of the hydroxyl group of S13 in T13S for participation in a pair of conventional hydrogen-bonding interactions (Figure 8). Why do the side chains of T13 and S13 adopt different low energy conformations? A rotation in χ to orient the hydroxyl group of T13 for formation of conventional hydrogen bonds with the carbonyl oxygen of R10 and the side chain of R17 as observed in T13S is prevented by the γ-methyl group of the side chain which would make a very unfavorable van der Waals contact with Y6 at 2.6 Å from the centroid of the aromatic ring. Thus, the on-face hydrogen bond observed in the native enzyme is enforced by a steric interaction which prevents the formation of two enthalpically more favorable conventional hydrogen bonds.

The results presented here suggest that functionally significant weakly polar interactions with the quadrapole of aromatic residues can be demonstrated experimentally. Competition with more numerous conventional hydrogen bonds may mitigate against their formation except in special circumstances where other structural constraints favor weakly polar interactions. The very fact that the interaction energies involved are small makes the detection of their influence on ligand binding or catalytic events particularly challenging.

REFERENCES

Armstrong, R. N. (1994) *Adv. Enzymol. Relat. Areas Mol. Biol. 69*, 1−44.

Atkins, W. M., Wang, R. W., Bird, A. W., Newton, D. J., & Lu, A. Y. H. (1993) *J. Biol. Chem. 268*, 19188−19191.

Bernstein, F. C., Koetzle, T. F., Williams, G. J. B., Meyer, E. F., Jr., Brice, M. D., Rogers, J. R., Kennard, O., Shimanouchi, T., & Tasumi, M. (1977) *J. Mol. Biol. 112*, 535−547.

Boys, S. F., & Bernardi, F. (1970) *Mol. Phys. 19*, 553−559.

Burley, S. K., & Petsko, G. A. (1986) *FEBS Lett. 203*, 139−143.

Burley, S. K., & Petsko, G. A. (1988) *Adv. Protein Chem. 39*, 125−189.

Chen, W.-J., Graminski, G. F., & Armstrong, R. N. (1988) *Biochemistry 27*, 647−654.

Cleland, W. W. (1979) *Methods Enzymol. 63*, 103−138.

Cowan, S. W., Newcomer, M. E., & Jones, T. A. (1993) *J. Mol. Biol. 230*, 1225−1246.

Demchenko, A. P. (1986) *Ultraviolet Spectroscopy of Proteins*, Springer-Verlag, Berlin.

Dirr, H., Reinemer, P., & Huber, R. (1994) *Eur. J. Biochem. 220*, 645−661.

Dougherty, D. A. (1996) *Science 271*, 163−168.

Frisch, M. J., Trucks, G. W., Head-Gordon, M., Gill, P. M. W., Wong, M. W., Foresman, J. B., Johnson, B. G., Schlegel, H. B., Robb, M. A., Replogle, E. S., Gomberts, R., Anders, J. L., Raghavachari, K., Binkley, J. S., Gonzalez, C., Martin, R. L., Fox, D. J., Defrees, D. J., Baker, J., Stewart, J. J. P., & Pople, J. A. (1992) *Gaussian 92*, Revision A, Gaussian, Inc., Pittsburgh, PA.

Furey, W. (1990) *Abstracts of the American Crystallographic Association Fortieth Anniversary Meeting*, New Orleans, LA, PA33.

Furey, W., Wang, B. C., & Sax, M. (1982) *J. Appl. Crystallogr. 15*, 160−166.

Garcia-Saez, I., Parraga, A., Phillips, M. F., Mantle, T. J., & Coll, M. (1994) *J. Mol. Biol. 237*, 298−314.

Graminski, G. F., Kubo, Y., & Armstrong, R. N. (1989) *Biochemistry 28*, 3562−3568.

Hendrickson, W. (1985a) *Methods Enzymol. 115*, 252−270.

Hendrickson, W. (1985b) *Crystallographic Computing 3: Data Collection, Structure Determination, Proteins, and Databases* (Sheldrick, G., Kruger, C., & Goddard, R., Eds.) pp 306−311, Clarendon Press, Oxford.

Hendrickson, W., & Konnert, J. (1980a) *Computing in Crystallography* (Diamond, R., Ramaseshan, S., & Venkatesan, K., Eds.) pp 1301−1323, Indian Academy of Sciences.

Hendrickson, W., & Konnert, J. (1980b) *Biomolecular Structure, Function, Conformation and Evolution* (Srinivasan, R., Ed.) Vol. 1, pp 43−57, Pergamon, Oxford.

Howard, A. J., Gilliland, G. L., Finzel, B. C., Poulos, T. L., Ohlendorf, D. H., & Salemme, F. R. (1987) *J. Appl. Crystallogr. 20*, 383−387.

Huskey, S.-E. W., Huskey, W. P., & Lu, A. Y. H. (1991) *J. Am. Chem. Soc. 113*, 2283−2290.

James, M. N. G., & Sielecki, A. R. (1983) *J. Mol. Biol. 163*, 299−361.

Jamison, R. S., Kakkad, B., Ebert, D. H., Newcomer, M. E., & Ong, D. E. (1995) *Biochemistry 34*, 11128−11132.
Ji, X., Zhang, P., Armstrong, R. N., & Gilliland, G. L. (1992) *Biochemistry 31*, 10169−10184.
Ji, X., Armstrong, R. N., & Gilliland, G. L. (1993) *Biochemistry 32*, 12949−12954.
Ji, X., Johnson, W. W., Sesay, M. A., Dickert, L., Prasad, S. M., Ammon, H. L., Armstrong, R. N., & Gilliland, G. L. (1994) *Biochemistry 33*, 1043−1052.
Ji, X., von Rosenvinge, E. C., Johnson, W. W., Tomarev, S. I., Piatigorsky, J., Armstrong, R. N., & Gilliland, G. L. (1995) *Biochemistry 34*, 5317−5328.
Johnson, W. W., Liu, S., Ji, X., Gilliland, G. L., & Armstrong, R. N. (1993) *J. Biol. Chem. 268*, 11508−11511.
Jones, T. A. (1978) *J. Appl. Crystallogr. 11*, 268−272
Jones, T. A., & Kjeldgaard, M. (1993) O Version 5.9.1, Department of Molecular Biology, BMC, Uppsala University, Sweden, and Department of Chemistry, Aarhus University, Denmark.
Jones, T. A., Zou, J.-Y., Cowan, S. W., & Kjeldgaard, M. (1991) *Acta Crystallogr. A47*, 110−119.
Karshikoff, A., Reinemer, P., Huber, R., & Ladenstein, R. (1993) *Eur. J. Biochem. 215*, 663−670.
Levitt, M., & Perutz, M. F. (1988) *J. Mol. Biol. 201*, 751−754.
Liu, S., Zhang, P., Ji, X., Johnson, W. W., Gilliland, G. L., & Armstrong, R. N. (1992) *J. Biol. Chem. 267*, 4296−4299.
Liu, S., Ji, X., Gilliland, G. L., Stevens, W. J., & Armstrong, R. N. (1993) *J. Am. Chem. Soc. 115*, 7910−7911.
Mannervik, B., Awasthi, Y. C., Board, P. G., Hayes, J. D., Di Ilio, C., Ketterer, B., Listowsky, I., Morgenstern, R., Muramatsu, M., Pearson, W. R., Pickett, C. B., Sato, K., Widersten, M., & Wolf, C. R. (1992) *Biochem. J. 282*, 305−308.
Mitchell, J. B. O., Nandi, C. L., McDonald, I. K., Thornton, J. L., & Price, S. L. (1994) *J. Mol. Biol. 239*, 315−331.
Parsons, J. F., & Armstrong, R. N. (1996) *J. Am. Chem. Soc. 118*, 2295−2296.
Pemble, S. E., & Taylor, J. B. (1992) *Biochem. J. 287*, 957−963.
Powell, M. J. D. (1977) *Mathematical Programming 12*, 241−254.
Reid, K. S. C., Lindley, P. F., & Thornton, J. M. (1985) *FEBS Lett. 190*, 209−213.
Reinemer, P., Dirr, H. W., Ladenstein, R., Schaffer, J., Gallay, O., & Huber, R. (1991) *EMBO J. 10*, 1997−2005.
Reinemer, P., Dirr, H. W., Ladenstein, R., Huber, R., Lo Bello, M., Federici, G. & Parker, M. W. (1992) *J. Mol. Biol. 227*, 214−226.
Rodham, D. A., Suzuki, S., Suenram, R. D., Lovas, F. J., Dasgupta, S., Goddard, W. A., III, & Blake, G. A. (1993) *Nature 362*, 735−737.
Singh, J., & Thornton, J. M. (1990) *J. Mol. Biol. 211*, 595−615.
Sinning, I., Kleywegt, G. J., Cowan, S. W., Reinemer, P., Dirr, H. W., Huber, R., Gilliland, G. L., Armstrong, R. N., Ji, X., Board, P. G., Olin, B., Mannervik, B., & Jones, T. A. (1993) *J. Mol. Biol. 232*, 192−212.
Sussman, J. L., Harel, M., Frolow, F., Oefner, C., Goldman, A., Toker, L., & Silman, I. (1991) *Science 253*, 872−879.
Suzuki, S., Green, P. G., Bumgarner, R. E., Dasgupta, S., Goddard, W. A., III, & Blake, G. A. (1992) *Science 257*, 942−945.
Thomas, K. A., Smoth, G. M., Thomas, T. M., & Feldman, R. J. (1982) *Proc. Natl. Acad. Sci. U.S.A. 79*, 4843−4847.
Waksman, G., Kominos, D., Robertson, S. C., Pant, N., Baltimore, D., Birge, R. B., Cowburm, D., Hanafusa, H., Mayer, B. J., & Overduin, M. (1992) *Nature 358*, 646−653.
Wilce, M. C. J., & Parker, M. W. (1994) *Biochim. Biophys. Acta 1205*, 1−18.
Wlodawer, A., Walter, J., Huber, R., & Sjolin, L. (1984) *J. Mol. Biol. 280*, 301−329.
Zhang, P., Graminski, G. F., & Armstrong, R. N. (1991) *J. Biol. Chem. 266*, 19475−19479.

BI960189K